Laminar Forced-Convective Heat Transfer with Varying Properties in the Entrance Region of Flat Rectangular Ducts

M. J. Maxwell and A. J. Ghajar

School of Mechanical and Aerospace Engineering, Oklahoma State University, Stillwater, Oklahoma 74078

Numerical results for air undergoing laminar forced-convective heat transfer in the entrance region of a flat rectangular duct with uniform wall temperature are obtained for uniform inlet velocity and temperature profiles. The coupled governing partial differential equations are solved in discretized form with property variations being updated through physical property relations. This enables the physical property and thermofluid solutions to converge simultaneously, resulting in a realistic solution to the governing equations. Constant-property results are also obtained, and Nusselt numbers of both the constant- and variable-property models are compared with those of other numerical computations. The results of the variable-property model are also compared with available experimental data. The variable-property results exhibit excellent correlation with the available experimental data. A sensitivity analysis is performed to determine the effects of individual property variations on local Nusselt numbers.

INTRODUCTION

A number of numerical studies of simultaneously developing laminar velocity and temperature fields in the entrance region of a tube or parallel-plate channel have appeared in the literature [1–13]. Such studies have been motivated by a growing interest in the application of compact heat exchangers where equivalent diameters are small, especially with gas flows, and the heat exchanger design range falls well within the low Reynolds number regime ($Re_d < 2300$). Kays [1] employed Langhaar's [2] velocity profiles to solve the combined entry length problem for Pr = 0.7 in a circular duct, and Goldberg [3] extended Kays' work for Prandtl numbers in the range 0.5 to 5.0. Ulrichson and Schmitz [4] obtained velocity and temperature profiles in the entrance region of a circular duct by calculating the radial velocity component from the continuity equation and Langhar's axial velocity profile for Pr = 0.7. The entry length problem was further refined by Hornbeck [5], who employed a finite-difference method for constant wall temperature and constant heat flux boundary conditions with Pr = 0.7, 2, and 5. Manohar [6] and Kakac and Özgü [7] studied the nonlinear equations for incompressible steady laminar flow heat transfer in the combined entrance region of a circular tube with boundary conditions similar to those of Hornbeck [5]. Sparrow [8] and Hwang and Fan [9] investigated the simultaneous development of velocity and temperature profiles for parallel-plate flow. Mercer et al. [10] based their results on refined momentum and energy equations, incorporating the stream function definition with a

finite-difference method. In addition, Mercer et al. [10] supplemented their analysis with experimental work to show how their numerical results compared. Narang and Hussain [11] took Hwang and Fan's [9] work one step further by including axial conduction and some transverse momentum.

In 1970 Bankston and McEligot [12] introduced a finite-difference solution that included property variations for the combined entrance region of a circular duct. Shumway and McEligot [13] extended the previous work to show significant variations in the properties of air for high heating rates through tube annuli.

Low Reynolds number flow conditions also prevail in noncompact heat exchangers with high-viscosity fluids. The analytical results for that case are presented in reference [14]; considered are variable-viscosity effects in the inlet region of circular tubes for both uniform heat flux and uniform wall temperature boundary conditions with Newtonian and pseudoplastic non-Newtonian liquids.

From this review of the literature it is evident that the combined entry length problem is a fundamental problem in heat transfer and fluid flow. However, these studies have not properly accounted for variations of properties when large wall-to-inlet temperature differences are present. The majority of these studies either neglect property variations of the fluid or correct the constant-property solutions for the variation of properties by using a reference temperature or property ratio scheme. However, the reference temperature and property ratio methods have been applied to only a fraction of the geometries and boundary conditions for which constant-property solutions are available. This is because the results must be correlated for a specific duct cross section, duct wall boundary condition, and flow orientation [14].

In applications such as gas-cooled nuclear reactors, large wall-to-inlet temperature differences ($T_w/T_e >> 1.1$) may occur in the entrance region between heat-transferring plates. These variations in temperature will affect the physical properties of the fluid, which in turn affect the development of the inlet velocity and temperature profiles. In this study a method for accurately predicting velocity and temperature profiles (which have a direct bearing on local heat transfer coefficients) is proposed for laminar forced-convective heat transfer with varying properties in the entrance region of flat rectangular ducts.

It should be noted that the analysis presented in this paper is not limited to the entrance region of flat rectangular ducts. The parallel-plate geometry is a limiting geometry for the family of rectangular and concentric annular ducts and lends itself to simple mathematical treatment. In most cases the results for the parallel-plate geometry form an upper bound on the fluid friction and heat transfer coefficients for these two classes of ducts.

This study combines physical property relations with a discretized method for solving the two-dimensional governing equations by utilizing the TEACH (teaching elliptic axisymmetric characteristics heuristically) computer program [15] to compute local Nusselt numbers in the entrance region between parallel flat plates. Patankar [16] gives an excellent outline for the discretized method used in the present paper. The implementation of boundary conditions for this discretized method is exemplified in Maxwell [17].

The present paper considers air (Pr ~ 0.7) as the fluid medium and the plates to be of constant uniform temperature. The properties of air were first considered to be constant and the results were compared with the numerical results of references [10] and [11]. Then the properties of air were allowed to vary and the variable-property results were compared with the experimental data of reference [10]. Finally, the effect of individual property variations on the local Nusselt numbers at various wall-to-inlet temperature ratios was studied.

ANALYSIS

The geometry under consideration is shown in Fig. 1. The two semi-infinite parallel plates of length L separated by a distance $2a$ are set to a constant uniform wall temperature T_w. The inlet velocity and temperature profiles of the air are uniform and of magnitude U_e and T_e, respectively.

The continuity, momentum, and energy equations governing the thermal flow field are

$$\frac{\partial}{\partial x}(\rho u) + \frac{\partial}{\partial y}(\rho v) = 0 \tag{1}$$

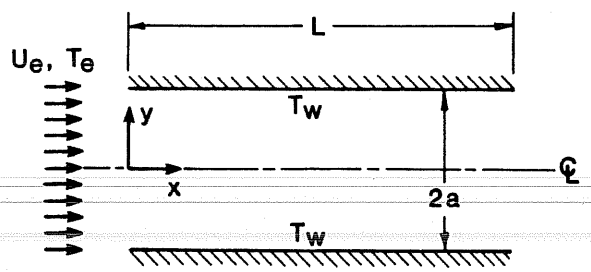

Figure 1 Geometry of the problem.

$$\frac{\partial}{\partial x}(\rho uu) + \frac{\partial}{\partial y}(\rho uv) - \frac{\partial}{\partial x}\left(\mu \frac{\partial u}{\partial x}\right) - \frac{\partial}{\partial y}\left(\mu \frac{\partial u}{\partial y}\right) = -\frac{\partial P}{\partial x} + S_u \quad (2)$$

$$\frac{\partial}{\partial x}(\rho uv) + \frac{\partial}{\partial y}(\rho vv) - \frac{\partial}{\partial x}\left(\mu \frac{\partial v}{\partial x}\right) - \frac{\partial}{\partial y}\left(\mu \frac{\partial v}{\partial y}\right) = -\frac{\partial P}{\partial y} + S_v \quad (3)$$

$$\frac{\partial}{\partial x}(\rho uT) + \frac{\partial}{\partial y}(\rho vT) - \frac{\partial}{\partial x}\left(\frac{k}{C_P}\frac{\partial T}{\partial x}\right) - \frac{\partial}{\partial y}\left(\frac{k}{C_P}\frac{\partial T}{\partial y}\right) = 0 \quad (4)$$

where

$$S_u = \frac{\partial}{\partial x}\left(\mu \frac{\partial u}{\partial x}\right) + \frac{\partial}{\partial y}\left(\mu \frac{\partial v}{\partial x}\right) \quad (2a)$$

$$S_v = \frac{\partial}{\partial x}\left(\mu \frac{\partial u}{\partial y}\right) + \frac{\partial}{\partial y}\left(\mu \frac{\partial v}{\partial y}\right) \quad (3a)$$

The properties are left within the derivatives to preserve the property variation effect.

Considering the thermal flow field to be symmetric about the duct centerline in Fig. 1, the boundary conditions are given as

$$u(0, y) = U_e \quad (5a)$$

$$\frac{\partial}{\partial x}[\rho u(L_\infty, y)] = 0 \quad (5b)$$

$$u(x,a) = 0, \qquad \frac{\partial}{\partial y}[\rho u(x,0)] = 0 \quad (5c)$$

$$v(0, y) = 0 \quad (6a)$$

$$v(L_\infty, y) = 0 \quad (6b)$$

$$v(x,a) = 0, \qquad v(x,0) = 0 \quad (6c)$$

$$T(0, y) = T_e \quad (7a)$$

$$\frac{\partial}{\partial x}[T(L_\infty, y)] = 0 \quad (7b)$$

$$T(x,a) = T_w, \qquad \frac{\partial}{\partial y}[T(x,0)] = 0 \quad (7c)$$

These boundary conditions were implemented in the TEACH code by the methods outlined in reference [17]. The TEACH code utilizes discretized functions developed from a control volume-based precept. These functions lend themselves to a coarse grid system for simple geometries. A staggered nonuniform grid system was employed, and the grid density was increased near the inlet and walls to account for high heating rates and large momentum changes. The number of grid points and the grid size were increased and decreased, respectively, until no appreciable change in Nu_x was detected at various x^+ locations. A 21 by 20 (x by y) expanding grid system was found to be suitable for the range of boundary parameters considered. The grid expanded from inlet to outlet and upper wall boundary to centerline.

The temperature and velocity fields were determined, and the local Nusselt numbers were calculated so that the results could be compared to both numerical and experimental results. The local Nusselt number Nu_x based on the mixed mean fluid temperature is given as

$$\mathrm{Nu}_x = \frac{hd}{k} = \frac{-4a}{T_w - T_m}\frac{\partial T}{\partial y}\bigg|_{y=a} \quad (8)$$

where

$$T_m = \frac{1}{A_c V \rho C_P}\int_{A_c} \rho C_P(uT)\, dA_c \quad (8a)$$

and

$$V = \frac{1}{A_c \rho}\int_{A_c} \rho u\, dA_c \quad (8b)$$

In order to compare the results of the present variable-property model with experimental data of Mercer et al. [10] the following local Nusselt number conversion relation was employed [17]:

$$\mathrm{Nu}_{\mathrm{lo}} = \frac{1}{2}\mathrm{Nu}_x\left(\frac{T_w - T_m}{T_w - T_e}\right) \quad (9)$$

This conversion was necessary because Mercer et al. defined their hydraulic diameter differently and based their local Nusselt number on the inlet fluid temperature.

The physical properties, k, μ, and C_P were computed using thermophysical property relations. Density ρ was computed from the ideal gas law. The thermophysical property update method intro-

duced in the TEACH code uses "new" or "updated" temperatures from the latest temperature grid sweep to compute physical properties of the fluid at each grid point. This enables the property and thermofluid solutions to converge simultaneously, resulting in a realistic solution of the governing Eqs. (1)–(4). The physical property equations of air used in the present analysis were taken directly from standard sources [18, 19].

Thermal conductivity [18]:

$$k = \frac{4186(6.325 \times 10^{-7} T^{1.5})}{T + 245.4 \times 10^{-12/T}} \text{ W/m K} \tag{10}$$

where T is in degrees Kelvin.

Viscosity [18]:

$$\mu = \frac{1.458 \times 10^{-6} T^{1.5}}{T + 110.4} \text{ kg/m s}^2 \tag{11}$$

where T is in degrees Kelvin.

Specific heat [19]:

For $250 < T \leq 600$ K

$$C_P = 4184(0.244388 - 4.20419 \times 10^{-5} T + 9.61128 \times 10^{-8} T^2 - 1.16383 \times 10^{-11} T^3) \text{ J/kg K} \tag{12a}$$

For $600 < T < 1500$ K

$$C_P = 4184(0.208831 + 7.71027 \times 10^{-5} T - 8.56726 \times 10^{-9} T^2 - 4.75772 \times 10^{-12} T^3) \text{ J/kg K} \tag{12b}$$

where T is in degrees Kelvin.

Density:

$$\rho = \frac{P}{287T} \text{ kg/m}^3 \tag{13}$$

where T is the absolute temperature in degrees Kelvin and pressure P is in pascals.

CONSTANT-PROPERTY RESULTS

Local Nusselt numbers based on the mixed mean fluid temperature [see Eq. (8)] of the present analysis are compared graphically with those of Narang and Hussain [11] for Re_d values of 20 and 1000 in Figs. 2 and 3, respectively. As expected, the computational technique has a large effect on the results

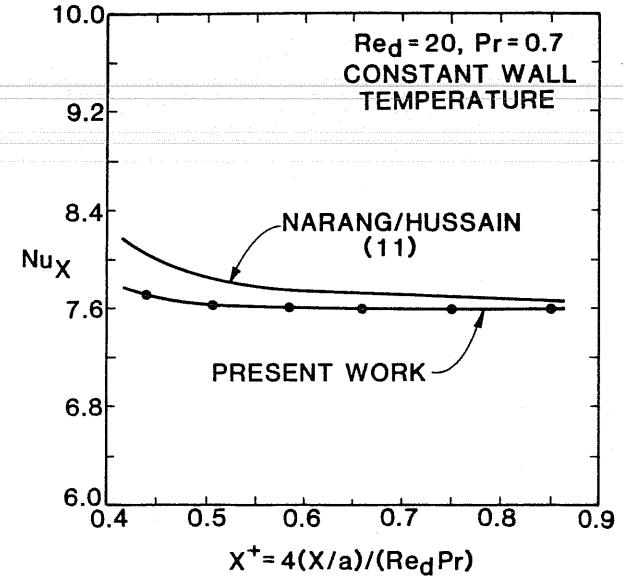

Figure 2 Comparison of constant-property results of the present study with results of Narang and Hussain [11] at $Re_d = 20$.

in the inlet region. For $Re_d = 20$ the present results are within 5% of those of Narang and Hussain. The present results also compare well with their results for $Re_d = 1000$ and $x^+ > 0.02$, but significant deviations between the results occur near the inlet ($x^+ < 0.02$). The inertia terms of the axial and transverse momentum equations in Narang and Hussain were linearized with the uniform inlet velocity, which allows no variation of the velocities (axial and transverse) in the inertia terms (i.e., $v\,\partial u/\partial y = v\,\partial v/\partial y = 0$). The deviations in the results near the inlet are attributed to this linearization of the inertia terms in reference [11].

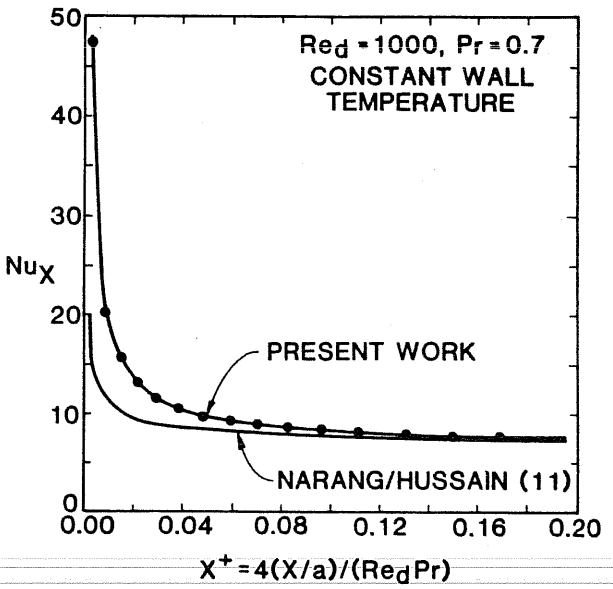

Figure 3 Comparison of constant-property results of the present study with results of Narang and Hussain [11] at $Re_d = 1000$.

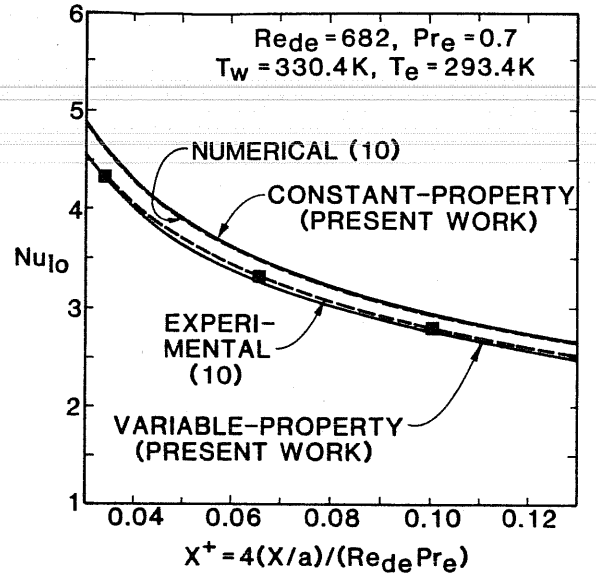

Figure 4 Comparison of constant- and variable-property results of the present study with numerical and experimental results of Mercer et al. [10] at Re_{de} = 682.

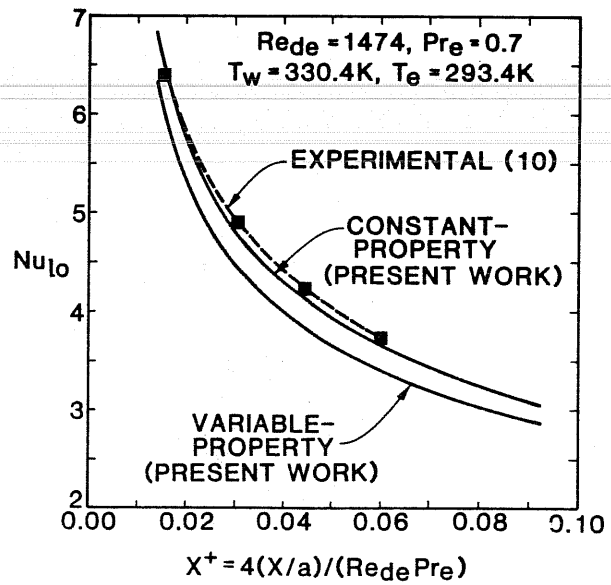

Figure 5 Comparison of constant- and variable-property results of the present study with experiments of Mercer et al. [10] at Re_{de} = 1474.

The constant-property results of the present work deviate only 2% from the numerical results of Mercer et al. [10] for Re_{de} = 682 and Pr_e = 0.7 (see Fig. 4). The present constant-property model also predicts the asymptotic $C_f Re_d$ and Nu_x for constant wall temperature given by Kays and Crawford [20] as 24.0 and 7.54, respectively.

VARIABLE-PROPERTY RESULTS

The properties were allowed to vary according to Eqs. (10)–(13). Since the inlet boundary conditions and inlet physical properties remain constant, the inlet Reynolds number Re_{de} and inlet Prandtl number Pr_e will be used to reference a particular variable-property case. The variable- and constant-property results are compared to the experimental results of Mercer et al. [10].

In the experimental analysis of Mercer et al. [10], both uniform plate temperatures were reported to be 330.4 K and the inlet air temperature was reported to vary during the days of testing from 291.5 to 297.0 K. The specific inlet air temperature corresponding to a specific test was not available in their paper. Therefore, a mean inlet air temperature of 294.3 K was assumed, and the local Nusselt numbers based on this inlet temperature [see Eq. (9)] were determined for inlet Reynolds numbers Re_{de} of 682 and 1474.

Present variable- and constant-property Nu_{lo} values are compared with the experimentally determined Nu_{lo} values of Mercer et al. in Figs. 4 and 5 for Re_{de} = 682 and 1474, respectively. The variable-property results are in excellent agreement with those of Mercer et al. for Re_{de} = 682. Constant- and variable-property results differ by approximately 6% for $x^+ < 0.07$.

For Re_{de} = 1474 and the assumed mean T_e = 294.3 K it would appear in Fig. 5 that either the variable-property model has failed to predict "correct" results or that some inconsistencies exist between the present model's boundary conditions and those of the experiments in Mercer et al. [10]. For an inlet temperature of 297.0 K the present variable-property results compare extremely well with those of reference [10] at Re_{de} = 1474, as shown in Fig. 6. The effect of inlet temperature on Nu_{lo} may be seen in Fig. 6.

The continuous curves presented in Fig. 6 are a result of the present variable-property model after converting Nu_x to Nu_{lo} at inlet temperatures of 291.5, 294.3, and 297.0 K. The reported results of Mercer et al. [10] also appear in Fig. 6. If the nondimen-

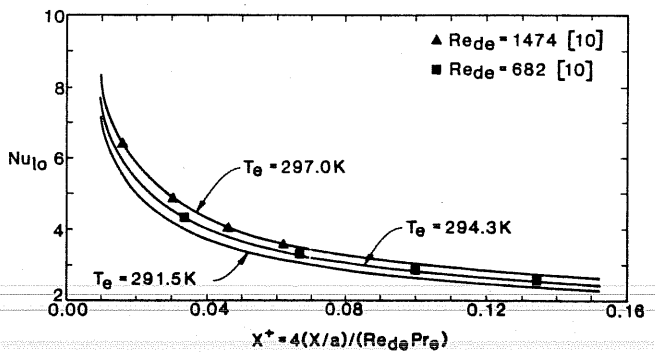

Figure 6 Effect of inlet temperature on variable-property results.

sional variables (Re_{de}, Pr_e, Nu_{lo}, Nu_x) were defined by fixed reference values (μ_e, U_e, ρ_e, C_{Pe}, k_e, h_e), the results of both the present work and reference [10] should appear as a continuous curve when the nondimensional heat transfer coefficient is plotted against a nondimensional entry length. It must be noted that deviations in inlet temperature will have more effect on an inlet-based Nusselt number than a mixed mean-based Nusselt number. The mixed mean Nusselt number or Nu_x is determined by a numerical integration scheme that has an averaging effect that diminishes entrance temperature effects.

The constant- and variable-property results differ by approximately 6% for a wall-to-inlet temperature ratio of 1.1. This is a noticeable but not a significant difference in local heat transfer coefficients. But for larger wall-to-inlet temperature ratios sufficiently large deviations in local heat transfer coefficients may warrant the use of a variable-property model.

The effect of high heating rates on Nu_x is most readily seen in Fig. 7. The dashed line in Fig. 7 represents the results of the constant-property model at Re_{de} = 682, T_e = 294.3 K, and T_w = 330.4, 700, and 1000 K. Note that there is only one curve representing the constant-property case for the three wall temperatures. Also seen in Fig. 7 are three solid curves labeled with wall temperature values. These curves show how higher heating rates ($T_w/T_e >>$ 1.1) cause the properties to vary in such a way as to produce a net decrease in the local Nusselt number with respect to the constant-property model. This shows that a constant-property model will produce unrealistic local Nusselt numbers compared to a variable-property model for large heating rates. The percent differences in Nu_x near the entrance for T_w = 330.4, 700, and 1000 K are 7, 34, and 44, respectively.

Figure 8 vividly displays the effects of high heating rates on the local friction coefficient. Again, there is only one curve representing the constant-property case for all three wall temperatures. The other three curves, labeled with wall temperature values, show how the variable-property results predict a higher local friction coefficient than do the constant-property results for high heating rates.

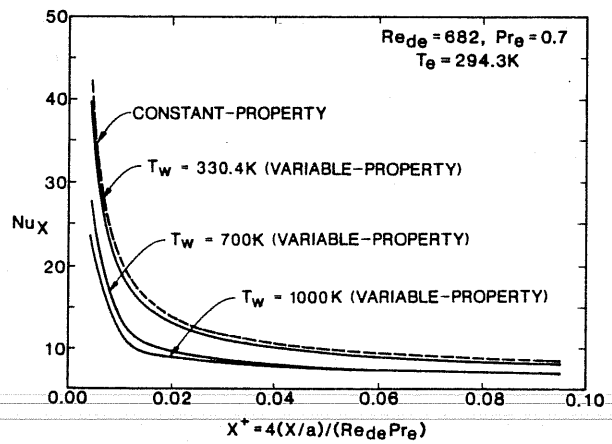

Figure 7 Effects of high heating rates on local Nusselt number.

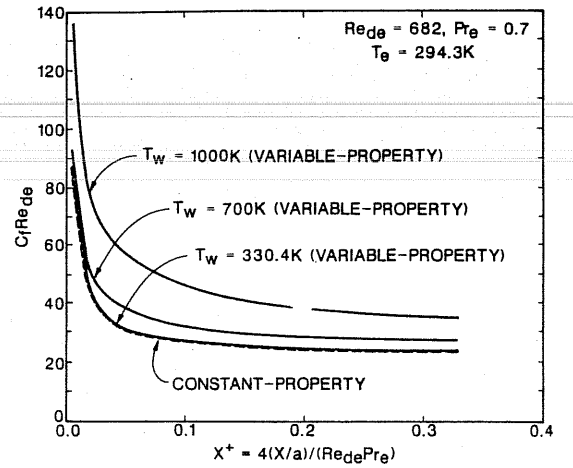

Figure 8 Effects of high heating rates on local friction coefficient.

A sensitivity analysis was also conducted [17], and the variation in the thermal conductivity k was found to have the greatest influence on Nu_x when heating rates were varied. Specific heat C_P caused an increase in Nu_x as heating rates were increased, but the combined effect of the other three properties (k, μ, ρ) in decreasing Nu_x caused a net reduction in Nu_x with increased heating rate. This indicates that it is important to correctly model the variation in thermal conductivity when considering internal convective heat transfer in air.

CONCLUSIONS

The results of the present constant-property model are in close agreement with those of other established constant-property models. The variable-property model was introduced in an attempt to ensure a more realistic solution for air undergoing laminar forced-convective heat transfer between parallel plates. The results of the present variable-property model are in better agreement than those of the constant-property model when compared to the experimental results of Mercer et al. [10]. The thermophysical property update method has been shown to exhibit realistic internal laminar convective heat transfer principles.

The method presented in this paper more correctly predicts internal forced-convective heat transfer by integrating physical property equations with

currently available discretization methods. By changing the physical property equations, other fluids undergoing internal forced-convective heat transfer may be modeled.

NOMENCLATURE

A_c cross-sectional area between parallel plates
a half-width between parallel plates, defined in Fig. 1
C_f local friction coefficient [$= (2/\rho V^2)\mu(\partial u/\partial y)_{y=a}$]
C_P specific heat at constant pressure
d hydraulic diameter ($= 4a$)
h local heat transfer coefficient
k thermal conductivity
L length of parallel plates in axial direction, defined in Fig. 1
L_∞ fully developed length
Nu_x local Nusselt number, defined by Eq. (8)
$\mathrm{Nu}_{\mathrm{lo}}$ local Nusselt number, defined by Eq. (9)
P pressure
Pr Prandtl number ($= \mu C_P/k$)
Pr_e inlet Prandtl number
Re_d Reynolds number based on hydraulic diameter ($= \rho u d/\mu$)
Re_{de} inlet Reynolds number
S_u general source term for u velocity, used in Eq. (2)
S_v general source term for v velocity, used in Eq. (3)
T local temperature
T_e inlet temperature
T_m mixed mean temperature, defined by Eq. (8*a*)
T_w wall temperature
U_e uniform inlet velocity
u local axial velocity
V average velocity, defined by Eq. (8*b*)
v local transverse velocity
x axial coordinate
x^+ nondimensional axial coordinate [$= 4(x/a)/(\mathrm{Re}_d\mathrm{Pr})$]
y transverse coordinate
ρ fluid density
μ fluid viscosity

REFERENCES

[1] Kays, W. M., Numerical Solutions for Laminar-Flow Heat Transfer in Circular Tubes, *Trans. ASME*, vol. 77, pp. 1265–1274, 1955.

[2] Langhaar, H. L., Steady Flow in the Transition Length of a Straight Tube, *Trans. ASME, J. Appl. Mech.*, vol. 64, pp. 4–55, 1942.

[3] Goldberg, P., A Digital Computer Solution for Laminar Flow Heat Transfer in Circular Tubes, M.S. thesis, Massachusetts Institute of Technology, Cambridge, 1958.

[4] Ulrichson, D. L. and Schmitz, R. A., Laminar-Flow Heat Transfer in the Entrance Region of Circular Tubes, *Int. J. Heat Mass Transfer*, vol. 8, pp. 253–258, 1965.

[5] Hornbeck, R. W., An All-Numerical Method for Heat Transfer in the Inlet of a Tube, ASME Paper 65-WA/HT-36, 1965.

[6] Manohar, R., Analysis of Laminar-Flow Heat Transfer in the Entrance Region of Circular Tubes, *Int. J. Heat Mass Transfer*, vol. 12, pp. 15–22, 1969.

[7] Kakac, S. and Özgü, M. R., Analysis of Laminar Flow Forced Convection Heat Transfer in the Entrance Region of a Circular Pipe, *Waerme Stoffuebertrag.*, vol. 2, pp. 240–245, 1969.

[8] Sparrow, E. M., Analysis of Laminar Forced-Convection Heat Transfer in the Entrance Region of Flat Rectangular Ducts, NACA Tech. Note TN 3331, 1955.

[9] Hwang, C. L. and Fan, L. T., Finite Difference Analysis of Forced-Convection Heat Transfer in Entrance Region of Flat Rectangular Duct, *Appl. Sci. Res. Sect. A*, vol. 13, 1964, pp. 401–422,

[10] Mercer, W. E., Pearce, W. M., and Hitchcock, J. E., Laminar Forced Convection in the Entrance Region between Flat Plates, *J. Heat Transfer*, vol. 89, pp. 251–257, 1967.

[11] Narang, B. S. and Hussain, N. A., Analysis of Laminar Forced Convection Heat Transfer in the Entrance Region of a Flat Duct with Uniform Wall Temperature, ASME Paper 81-HT-29, 1981.

[12] Bankston, C. A. and McEligot, D. M., Turbulent and Laminar Heat Transfer to Gases with Varying Properties in the Entry Region of Circular Ducts, *Int. J. Heat Mass Transfer*, vol. 13, pp. 319–344, 1970.

[13] Shumway, R. M. and McEligot, D. M., Heated Laminar Gas Flow in Annuli with Temperature Dependent Transport Properties, *Nucl. Sci. Eng.*, vol. 46, pp. 394–407, 1971.

[14] Bergles, A. E., Prediction of the Effects of Temperature-Dependent Fluid Properties on Laminar Heat Transfer, in *Low Reynolds Number Flow Heat Exchangers*, S. Kakac, R. K. Shaw, and A. E. Bergles, eds., pp. 451–471, Hemisphere, Washington, D.C., 1983.

[15] Gosman, A. D. and Pun, W. M., Calculation of Recirculating Flows, Report HTS/74/2, Dept. of Mechanical Engineering, Imperial College, London, 1974.

[16] Patankar, S. V., *Numerical Heat Transfer and Fluid Flow*, Hemisphere, Washington, D.C., 1980.

[17] Maxwell, M. J., Computer Simulation of Laminar Forced Convective Heat Transfer in the Entrance Region of a Straight Channel for Constant- and Variable-Property Gases, M.S. thesis, School of Mechanical and Aerospace Engineering, Oklahoma State University, Stillwater, 1985.

[18] Bolz, R. E. and Tuve, G. L. (eds.), *CRC Handbook of Tables for Applied Engineering Science*, 2d ed., p. 651, CRC Press, Boca Raton, Fla., 1976.

[19] Touloukian, Y. S., and Makita, T., Thermophysical Properties of Matter. In Y. S. Touloukian et al. (eds.), *Specific Heat: Nonmetallic Liquids and Gases*, vol. 6, p. 293. Thermophysical Properties Research Center Data Series, Plenum, New York, 1970.

[20] Kays, W. M. and Crawford, M. E., *Convective Heat and Mass Transfer*, 2d ed., McGraw-Hill, New York, 1980.

M. J. Maxwell is a mechanical engineer at General Dynamics, Fort Worth, Texas, where he has been since May 1985. He received his B.S. (1983), and M.S. (1985) in mechanical engineering from Oklahoma State University, Stillwater, Oklahoma.

A. J. Ghajar is an associate professor of mechanical and aerospace engineering at Oklahoma State University, where he has been since 1981. He received his B.S. (1974), M.S. (1975), and Ph.D. (1979) in mechanical engineering from Oklahoma State University. His research activities have been in the area of energy conversion, experimental and computational heat transfer and fluid flow, and development of variable fluid property heat transfer correlations.